Bioorganic & Medicinal Chemistry xxx (2016) xxx–xxx

Contents lists available at ScienceDirect

Bioorganic & Medicinal Chemistry

journal homepage: www.elsevier.com/locate/bmc

# Ferulic acid–carbazole hybrid compounds: Combination of cholinesterase inhibition, antioxidant and neuroprotection as multifunctional anti-Alzheimer agents

Lei Fang [a,b], Mohao Chen [a], Zhikun Liu [a,c], Xubin Fang [a], Shaohua Gou [a,*], Li Chen [c,*]

[a] Jiangsu Province Hi-Tech Key Laboratory for Bio-medical Research and School of Chemistry and Chemical Engineering, Southeast University, Nanjing 211189, China
[b] State Key Laboratory of Natural Medicines, China Pharmaceutical University, Nanjing 210009, China
[c] Department of Natural Medicinal Chemistry, China Pharmaceutical University, Nanjing 210009, China

ARTICLE INFO

*Article history:*
Received 5 November 2015
Revised 5 January 2016
Accepted 7 January 2016
Available online xxxx

*Keywords:*
Hybrid compounds
Antioxidant
Anti-Alzheimer
AChE inhibitor

ABSTRACT

In order to search for novel multifunctional anti-Alzheimer agents, a series of ferulic acid–carbazole hybrid compounds were designed and synthesized. Ellman's assay revealed that the hybrid compounds showed moderate to potent inhibitory activity against the cholinesterases. Particularly, the AChE inhibition potency of compound **5k** ($IC_{50}$ 1.9 μM) was even 5-fold higher than that of galantamine. In addition, the target compounds showed pronounced antioxidant ability and neuroprotective property, especially against the ROS-induced toxicity. Notably, the neuroprotective effect of **5k** was obviously superior to that of the mixture of ferulic acid and carbazole, indicating the therapeutic effect of the hybrid compound is better than the combination administration of the corresponding mixture.



## 1. Introduction

Alzheimer's disease (AD) is a neurodegenerative and life-threatening disease characteristic of a progressive impairment of cognitive functions, behavioral disturbances and a decreasing ability to perform basic activities of daily living. Though the disease has been identified for more than 100 years, it is still incurable due to its complex pathogenesis. Substantial evidences have revealed that AD is a multifactorial syndrome derived from a complex array of neurochemical factors, involving the deficiency of synaptic acetylcholine and other related neurotransmitters, the formation of neurotoxic beta-amyloid (Aβ) peptide, oxidative stress, the inflammation of neurons, and so on.[1,2] Nowadays, only three acetylcholinesterase inhibitors (AChEIs), including galantamine, rivastigmine and donepenzil, and one *N*-methyl-D-aspartic acid receptor antagonist memantine are clinically available for the treatment of AD. The oldest AChEI tacrine was withdrawn from the market due to its serious hepatotoxicity. Notably, though AChEIs can enhance the level of synaptic acetylcholine (ACh) and consequently improve the cholinergic function in the central nervous system, they cannot halt the progression of AD and thereby only a symptom-ameliorating effect can be obtained.

Facing the complex etiology of AD, developing novel agents with multiple pharmacological effects has become a promising strategy in the search for new anti-AD agents. In this context, hybrid molecules, which consist of two or more pharmacophores in one molecule and could simultaneously target different pathogenic factors of AD, have attracted more and more attention. Carbazole derivatives have been reported to be able to inhibit the aggregation of Aβ which is one of the neuropathology characteristics of AD and plays a key role in triggering a neurotoxic cascade.[3] Before long, we also found that 2,8-disubstituted carbazole derivatives (e.g., **1a**), which could be regarded as the D-ring opened analogs of galantamine, could inhibit cholinesterase (ChE) and protect neurons from the toxicity induced by Aβ oligomers.[4] These unique characters of carbazole derivatives make them ideal lead structures for developing multifunctional anti-AD agents. Reactive oxygen species (ROS) are now regarded as another major etiological factor of AD since it is confirmed that ROS relate to formation of both amyloid plaques and neurofibrillary tangles, which are two major pathological hallmarks of AD.[5] Natural antioxidant ferulic acid (FA) could effectively scavenge ROS and exert protective effect on neurons against the ROS-induced toxicity in vitro, suggesting it may be useful for the treatment of AD.[6] Thereby, in order to take advantage of these two scaffolds, we have designed and synthesized a series of FA–carbazole hybrid compounds which contain the carbazole moiety connected to the carboxylic acid group of FA via an amide bond (Fig. 1). We hypothesized that the hybrid

* Corresponding authors. Tel./fax: +86 25 83272381
*E-mail addresses:* sgou@seu.edu.cn (S. Gou), chenliduo12@gmail.com (L. Chen).

http://dx.doi.org/10.1016/j.bmc.2016.01.010
0968-0896/

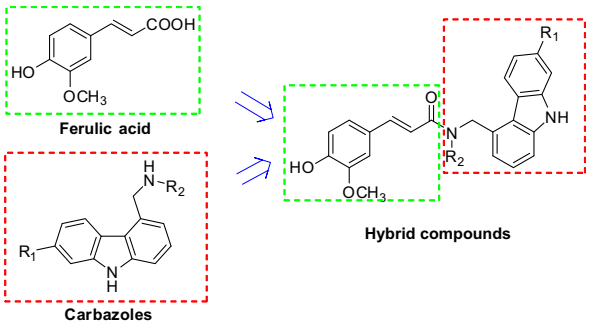


**Figure 1.** Drug design rationale of the target compounds.

compounds could simultaneously possess the ChE inhibition activity from the carbazole scaffold and the antioxidant and neuroprotective activity from the FA scaffold, and as a consequence, novel multifunctional anti-AD agents could be obtained.

## 2. Results and discussion

### 2.1. Chemistry

The synthesis of FA–carbazole hybrids **5a**–**k** was outlined in Schemes 1 and 2. Firstly, the carbazole derivatives **1a**–**k** were successfully prepared using our previously reported method (Scheme 1).[4] Then, the phenol hydroxyl functional group of FA was protected by acylation with ethyl carbonochloridate to give the ester **2**, which was further reacted with oxalyl chloride to form the acyl chloride intermediate **3**. Thereafter, compounds **4a**–**k** were synthesized by treating **3** with **1a**–**k** in the presence of pyridine, respectively. Finally, the protection group was removed by the treatment with aminoethanol in 95% ethanol aqueous solution to yield the target compounds **5a**–**k** (Scheme 2).

### 2.2. Cholinesterase inhibition

The deficiency of synaptic ACh and other related neurotransmitters is one of most important etiological factors of AD. In order to compensate ACh in the brain of AD patients, AChEIs have been developed and acting as the mainstay for the symptomatic treatment of AD. Since our former study revealed that 2,8-disubstituted carbazole derivatives could inhibit cholinesterases, we wondered whether the hybrid compounds retained such activity. Thus, the hybrid compounds were screened for the cholinesterase inhibitory activity in vitro by Ellman's assay. The results (Table 1) turned out that most of the synthesized compounds (except **5d**, **5e**, **5h**–**j**) showed moderate to potent inhibitory effect on the AChE, with $IC_{50}$ values ranging from 1.9 to 88.2 μM. Notably, the potency of compounds **1k** and **5k** was even higher than that of galantamine. Considering AChEs from different enzyme sources show significant structural difference, we further tested the inhibition effect of **1f**, **1k**, **5f**, and **5k** on human AChE. The results turned out that all of the four compounds showed potent inhibitory activity with $IC_{50}$ values from 5.1 to 22.0 μM is at the same level of the potency against AChE from Electric Eel. Analyzing the structure–activity relationship we found that the substituents $R_1$ and $R_2$ had important influence on the activity. When $R_2$ was ethyl (e.g., **5g**) or isopropyl (e.g., **5f**) which had a relative small size, the target compounds showed good activity. When the size of $R_2$ increased, the activity obviously reduced, indicating small alkyl substituents were optimal for the activity. Besides, the electric effect of $R_1$ also played an important role in the activity. Replacing the electron-donating methoxyl group with electron-accepting chlorine atom significantly improved the inhibitory activity, indicating the electron-withdrawing substituents could make a contribution to the activity. As for the butyrylcholinesterase (BChE), the activity levels of all compounds against BChE were generally higher than those against AChE with $IC_{50}$ values varying from 1.9 to 25.9 μM. Besides, the potency difference was also observed between the hAChE and hBChE groups. The difference of the activity against these two isoenzymes may origin from the structural difference of the isoenzymes. It was reported that at the midgorge level several aromatic residues of AChE are replaced by smaller aliphatic ones in BChE, which leads to the larger void along the BChE gorge with respect to AChE.[7]

### 2.3. Molecular modeling and ADME prediction

In order to investigate the interaction mode of the synthesized compounds with the target enzymes, we further performed molecular modeling study. It was revealed that the large active gorge of BChE allowed the ligands with large steric hindrance (e.g., **5i**) to enter the pocket and interact with the corresponding residues, whereas in the case of AChE the large steric hindrance of the

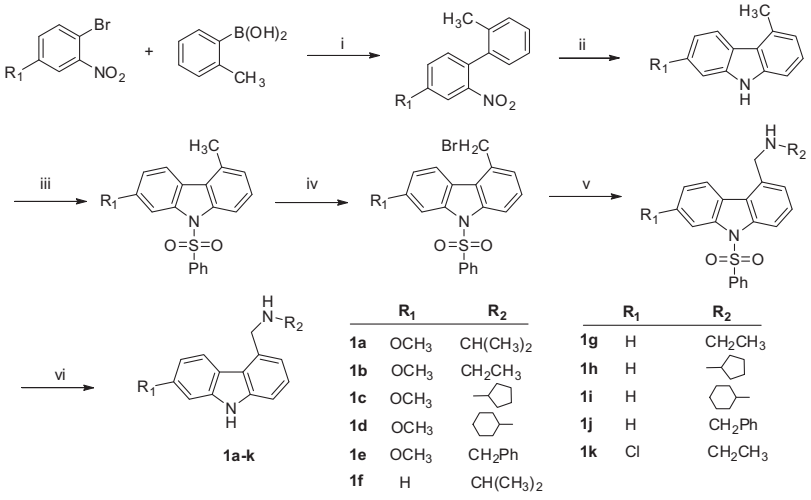


**Scheme 1.** The synthetic procedure of compounds **1a**–**k**. Regents and condition: (i) $Na_2CO_3$, $Pd(PPh_3)_4$, DME, reflux, 20 h; (ii) $PPh_3$, DCB, reflux, 3 h; (iii) $PhSO_2Cl$, NaH, THF, 0 °C/rt, overnight; (iv) NBS, AIBN, $CCl_4$, reflux, 3 h; (v) alkylamine, KI, $K_2CO_3$, anhydrous acetone, rt, overnight; (vi) 2 N NaOH, ethanol, reflux, overnight.

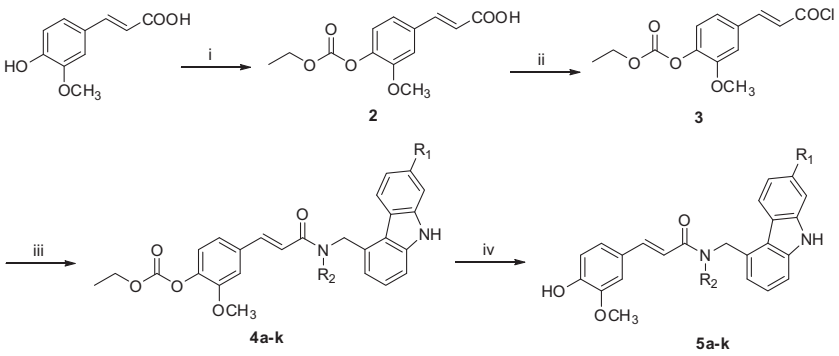


**Scheme 2.** The synthetic procedure of the target compounds **5a–k**. Regents and condition: (i) EtOCOCl, NaOH, $H_2O$, rt, 0.5 h; (ii) oxalyl chloride, $CH_2Cl_2$, DMF, −5 °C, 1 h; (iii) **1a–k**, pyridine, $CH_2Cl_2$, 0 °C,1 h; (iv) $NH_2CH_2CH_2OH$, 95% EtOH, rt.

**Table 1**
Inhibitory effect of **1b**, **1f**, **1k**, **5a–k** and galantamine (abbreviated as **Gal.**) on AChE and BChE ($IC_{50}$ values)

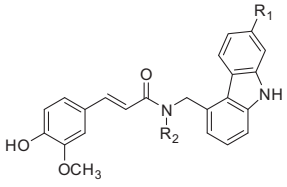


5a-k

| Compd | $R_1$ | $R_2$ | $IC_{50}$ ± SEM[a] (μM) | | | |
|---|---|---|---|---|---|---|
| | | | AChE[b] | hAChE[e] | BChE[b] | hBChE[e] |
| **Gal.** | — | — | 8.5 ± 1.5 | | 28.1 ± 6.2 | |
| **1a** | —$OCH_3$ | —$CH(CH_3)_2$ | 50.8 ± 12.1[c] | | 10.1 ± 7.7[c] | |
| **1f** | —H | —$CH(CH_3)_2$ | 21.6 ± 7.2 | 18.0 ± 2.1 | 8.9 ± 2.0 | 8.1 ± 1.1 |
| **1k** | —Cl | —$CH_2CH_3$ | 2.1 ± 0.6 | 5.1 ± 0.8 | 1.9 ± 0.2 | 7.9 ± 0.5 |
| **5a** | —$OCH_3$ | —$CH(CH_3)_2$ | 58.2 ± 11.2 | | 13.9 ± 2.6 | |
| **5b** | —$OCH_3$ | —$CH_2CH_3$ | 61.6 ± 13.8 | | 19.8 ± 4.2 | |
| **5c** | —$OCH_3$ |  | 88.2 ± 17.1 | | 25.9 ± 9.3 | |
| **5d** | —$OCH_3$ |  | >100 | | 20.5 ± 3.2 | |
| **5e** | —$OCH_3$ | —$CH_2Ph$ | >100 | | n.d.[d] | |
| **5f** | —H | —$CH(CH_3)_2$ | 11.1 ± 2.4 | 22.0 ± 4.0 | 12.7 ± 1.3 | 9.0 ± 2.1 |
| **5g** | —H | —$CH_2CH_3$ | 18.0 ± 1.9 | | 13.8 ± 2.8 | |
| **5h** | —H |  | >100 | | 31.6 ± 11.4 | |
| **5i** | —H |  | >100 | | 22.0 ± 2.5 | |
| **5j** | —H | —$CH_2Ph$ | >100 | | n.d.[d] | |
| **5k** | —Cl | —$CH_2CH_3$ | 1.9 ± 0.8 | 6.9 ± 0.9 | 3.1 ± 0.4 | 2.8 ± 0.4 |

[a] Data are the mean values of at least three determinations.
[b] AChE from Electric Eel and BChE from equine serum were used.
[c] Values are cited from Ref. 4.
[d] n.d. Means not determined.
[e] Human AChE and BChE were used.

cyclohexyl group of **5i** totally blocked the interactions (Fig. 2A and B). In contrast, compound **5k** whose $R_2$ is a small ethyl group could effectively enter the active pocket of AChE and interact with the key residue Trp84 through a π–π interaction (Fig. 2C). Its interaction mode is similar to that of galantamine.[8]

Given the target compounds were designed for the treatment of the central nervous system disease, the physicochemical properties such as Clog*p* and blood–brain barrier (BBB) penetration ability were essential for the drug-likeness of the target compounds. Thereby, ADMET of **5k** was predicted using ADMET predictor 7.0 (Table 2). It was found that the Clog*p* of **5k** is 4.39. This value is higher than that of tacrine but still within the range given by Lipinski's Rule of Five which suggests the optimal log*p* value of drug candidate should be not higher than 5. The high Clog*p* value indicates a good lipophilicity of the target compound. Though the high lipophilicity decreases the aqueous solubility of **5k** as compared with tacrine, it guarantees a good ability of the target compound to penetrate BBB, which was also confirmed by the prediction.

## 2.4. Free radical scavenging activity

The antioxidant effect is believed to be responsible for the anti-AD property of FA. Thereby, using the UV spectroscopy method,[9] the capacity of different concentrations (1, 2, 10, 50, 100 μM) of the target compounds to eliminate 2,2-diphenyl-1-picrylhydrazyl free radical (DPPH) as well as galvinoxyl radicals was determined

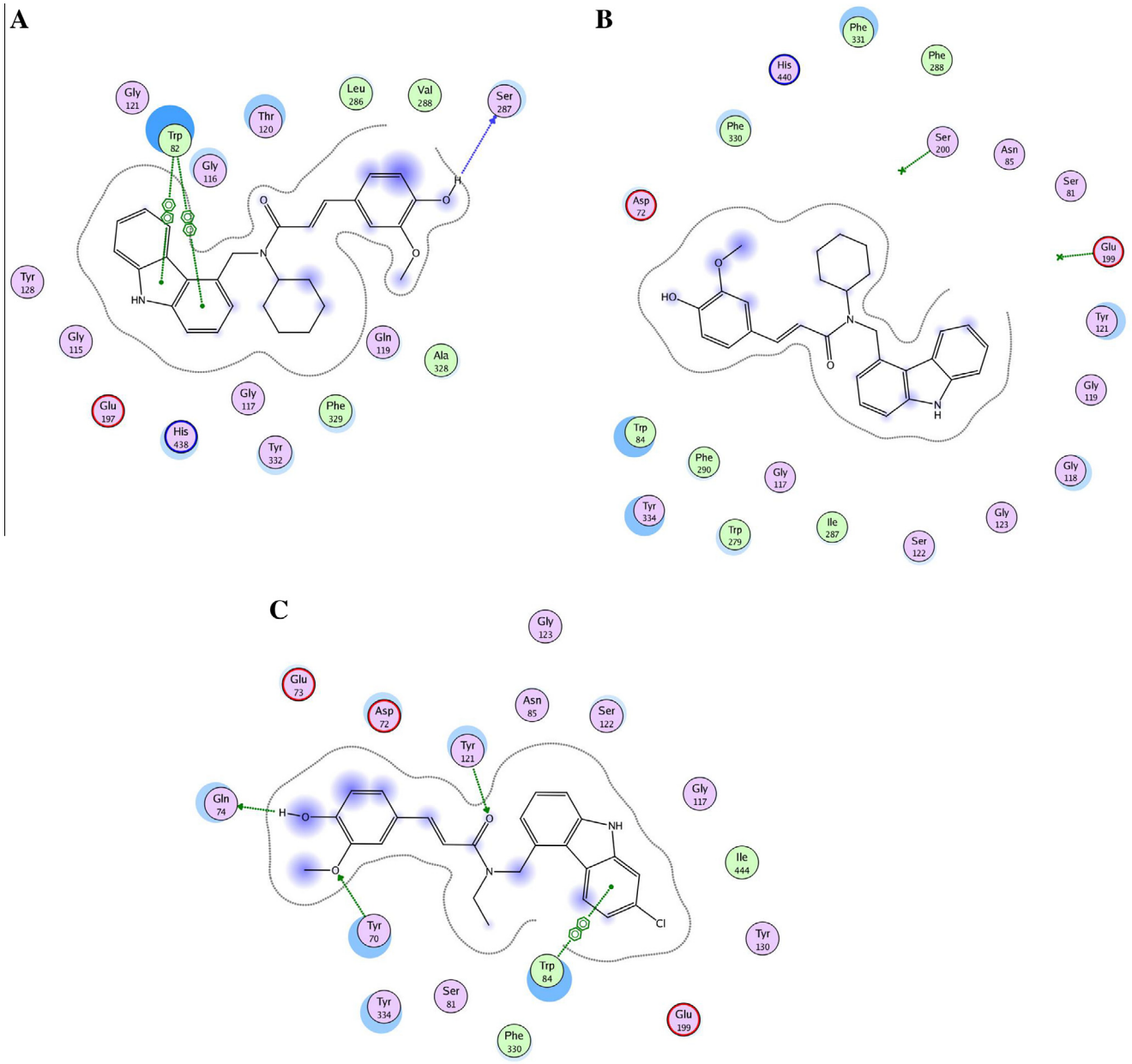


**Figure 2.** (A) The interaction of **5i** and BChE (Protein Data Bank code 1P0P); (B) the interaction of **5i** and AChE (Protein Data Bank code 3I6M); (C) the interaction of **5k** and AChE (Protein Data Bank code 3I6M). The pictures were generated from MOE.

**Table 2**
The ADMET prediction results of **5k** and tacrine

| Properties | **5k** | Tacrine |
|---|---|---|
| Clog p | 4.39 | 2.79 |
| $pK_a$ | 11.91, 9.02 | 10.06 |
| Solubility[a] | $1.14 \times 10^{-3}$ | $4.71 \times 10^{-1}$ |
| MDCK[b] | 270.51 | 353.51 |
| BBB penetration[c] | High | High |
| ADMET risk[d] | 6.16 | 5.45 |
| Toxicity[e] | hE, Hp | ra, SG, Hp, Mu |

[a] Water solubility (mg/mL).
[b] MDCK permeability (cm/s $\times 10^7$).
[c] Likelyhood of blood–brain barrier penetration.
[d] A score in the 0–24 range indicating the number of potential ADMET problems a compound might have. The higher the number is, the higher risk of a compound is.
[e] hE = hERG, SG = SGOT and SGPT evaluation, Hp = hepatotoxicity, ra = acute rat toxicity, Mu = ames positive.

in vitro. The free radical scavenging activity (FRSA) of the mixture of **1k** and FA (molar ratio: 1:1), which can be considered as corresponding bioactive components of the hybrid compound, was also tested for the comparison of the activity of the hybrid compound and the combination administration of the corresponding mixture. The results were shown in Tables 3 and 4. It was found that all of the tested compounds could effectively scavenge the free radicals. Similar to the action manner of FA, the FRSA of the target compounds against DPPH (Table 3) was generally higher than that against the galvinoxyl radicals (Table 4). As for DPPH, even at the lowest concentration (i.e., 1 μM), the DPPH FRSA% of the target compounds reached 20–40%; in contrast, the galvinoxyl FRSA% of the same compounds at 1 μM was only in the range of 1.1–25.9%. Our former study revealed that the different potency against these two radicals may probably be attributed to the fact that DPPH and galvinoxyl radicals belong to two different types of radicals: DPPH is a kind of typical nitrogen radicals while

**Table 3**
In vitro DPPH free radical scavenging activity (FRSA) of the target compounds

| Compd | DPPH FRSA%[a] | | | | |
|---|---|---|---|---|---|
| | 100 μm | 50 μm | 10 μm | 2 μm | 1 μm |
| **5a** | 98.0 ± 2.1 | 72.9 ± 5.1 | 68.2 ± 5.0 | 55.0 ± 7.7 | 45.1 ± 4.7 |
| **5b** | 94.9 ± 6.0 | 86.4 ± 8.3 | 71.3 ± 2.1 | 59.2 ± 5.5 | 33.1 ± 4.6 |
| **5c** | 90.4 ± 7.9 | 86.8 ± 5.9 | 67.4 ± 9.1 | 54.0 ± 7.7 | 34.8 ± 3.3 |
| **5d** | 88.6 ± 10.1 | 82.0 ± 8.6 | 50.9 ± 3.9 | 47.9 ± 1.8 | 38.6 ± 1.6 |
| **5f** | 90.9 ± 2.8 | 84.5 ± 2.9 | 68.9 ± 3.5 | 56.2 ± 6.0 | 44.1 ± 5.1 |
| **5g** | 86.3 ± 7.2 | 82.8 ± 8.0 | 55.0 ± 4.1 | 40.1 ± 2.2 | 24.7 ± 1.6 |
| **5h** | 90.3 ± 2.7 | 85.7 ± 5.2 | 66.6 ± 7.9 | 54.5 ± 4.2 | 25.9 ± 2.0 |
| **5i** | 89.2 ± 7.2 | 72.0 ± 7.6 | 63.1 ± 7.2 | 52.4 ± 8.7 | 30.3 ± 2.9 |
| **5k** | 91.9 ± 8.0 | 77.3 ± 2.3 | 66.0 ± 5.1 | 49.1 ± 7.7 | 41.8 ± 4.2 |
| **1k + FA** | 93.2 ± 2.0 | 71.4 ± 1.7 | 60.1 ± 3.0 | 44.7 ± 4.3 | 31.6 ± 2.1 |
| **FA** | 92.2 ± 7.0 | 72.0 ± 9.2 | 63.1 ± 5.5 | 44.4 ± 2.1 | 30.3 ± 6.0 |

[a] Data are the mean values ± SEM ($n$ = 3).

galvinoxyl radicals belong to reactive oxygen species. From a chemical point of view, DPPH radicals are more reactive than galvinoxyl radicals, and more easily captured by phenolic hydroxy groups which are responsible for the antioxidant activity of FA.[4] As for the mixture of **1k** and FA, it was found that the performance of the mixture was similar to FA, but showed a relative low FRSA as compared with **5k**. As far as the $R_1$ and $R_2$ groups are concerned, they seem have little effect on the antioxidant activity of the target compounds. When the substituents were changed, no obvious change of the FRSA was observed. This finding suggested that the antioxidant effect of the target compounds may originate from the FA moiety.

## 2.5. Neuroprotective effect

Both FA and the carbazole derivatives have been reported to possess neuroprotective effects.[3,4] Given the newly synthesized compounds are hybrid compounds from FA and carbazoles, it may be interesting to investigate whether these hybrid compounds could protect neurons from the exogenous toxins. Thus, using $H_2O_2$ or Aβ42 as the toxins, the neuroprotective effect of compound **5k** was determined in vitro by MTT assay.[4,10] For the comparison, the protective effect of the mixture of **1k** and FA (molar ratio: 1:1) was also measured. The results were shown in Figure 3. When PC12 cells were incubated with different concentrations of compound **5k** (0.1, 1, 10, 50 μM) for 24 h, no cytotoxicity was observed as compared with the vehicle group. In contrast, when the cells were treated with $H_2O_2$ (200 μM) or Aβ42 (5 μM), a significant toxicity to PC12 cells was observed as the viability of the cells dropped from 1.0 to 0.42 and 0.54, respectively. Interestingly, when PC12 cells were co-treated with compound **5k** (0.1, 1, 10, 50 μM), the induced toxicity was significantly alleviated in a dose-dependent manner, indicating compound **5k** could effectively protect the neurons from the exogenous toxin. It was noticed that the protective effect of compound **5k** against the $H_2O_2$-induced toxicity was higher than that against Aβ42-induced toxicity. $H_2O_2$ is well known for its oxidative damage while the toxicity caused by Aβ42 is more complex, which includes the generation of abnormally high concentration of reactive oxygen species, activating the release of damaging cytokines (e.g., interleukin-1, interleukin-6, TNF-α), and causing mitochondrial dysfunctions.[11] The protective effect of **5k** against Aβ42-induced toxicity may originate from the carbazole part as our former study revealed this scaffold could inhibit the aggregation of Aβ and exert neuroprotective effect. In contrast, the high protective potency against the $H_2O_2$-induced toxicity suggested that the antioxidant property, which was mainly contributed to the FA moiety, also played important roles in the neuroprotective effect of the target compound.

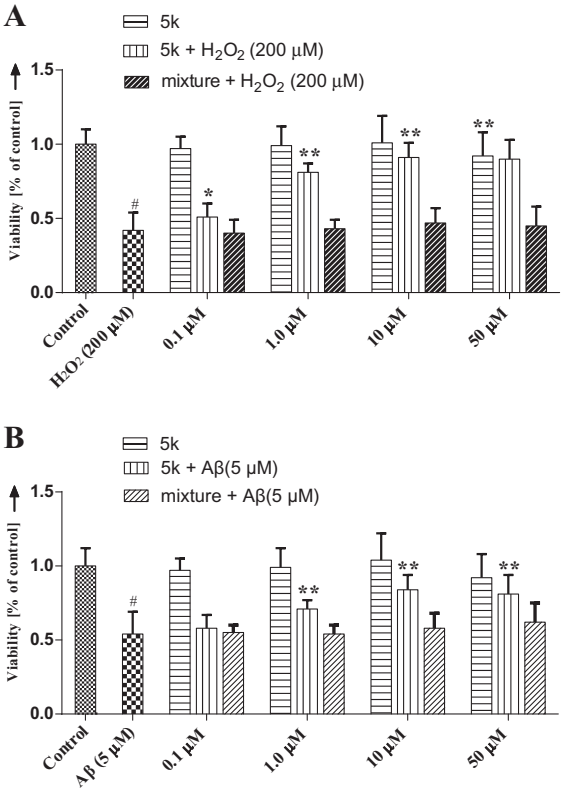


**Figure 3.** The neuroprotective effect of **5k** and its corresponding mixture (**1k** + **FA**, molar ratio: 1:1) against the $H_2O_2$ (A) or Aβ42 (B) induced toxicity. $^{\#}p$ <0.01 versus control, $^{*}p$ <0.05 versus Aβ (5 μM), $^{**}p$ <0.01 versus Aβ (5 μM), $n$ = 3.

As far as the mixture of **1k** and FA (molar ratio: 1:1) was concerned, only a slight protective effect against the Aβ42-induced toxicity was observed. In the $H_2O_2$ assay, the mixture showed no obvious difference from the vehicle group. These results strongly support that the combination of equimolar parts of FA and carbazole derivative in one hybrid molecule is clearly superior to a simple mixture of both parts.

**Table 4**
In vitro galvinoxyl free radical scavenging activity (FRSA) of the target compounds

| Compd | Galvinoxyl FRSA%[a] | | | | |
|---|---|---|---|---|---|
| | 100 μm | 20 μm | 10 μm | 2 μm | 1 μm |
| **5a** | 87.2 ± 9.0 | 51.7 ± 7.5 | 23.4 ± 4.2 | 8.0 ± 3.1 | 1.1 ± 0.7 |
| **5b** | 91.9 ± 6.7 | 78.2 ± 3.9 | 40.3 ± 4.8 | 29.2 ± 3.1 | 11.1 ± 1.2 |
| **5c** | 87.4 ± 11.7 | 66.8 ± 8.1 | 37.4 ± 6.2 | 24.0 ± 5.5 | 14.8 ± 2.7 |
| **5d** | 88.6 ± 6.3 | 72.0 ± 7.7 | 50.9 ± 5.9 | 40.9 ± 5.0 | 25.6 ± 1.5 |
| **5f** | 90.8 ± 9.7 | 87.5 ± 8.4 | 68.0 ± 7.3 | 55.2 ± 7.0 | 24.1 ± 2.7 |
| **5g** | 86.3 ± 7.0 | 82.8 ± 7.2 | 55.0 ± 3.2 | 40.1 ± 5.7 | 24.7 ± 2.0 |
| **5h** | 90.3 ± 7.6 | 85.7 ± 3.9 | 66.6 ± 6.7 | 54.5 ± 5.4 | 25.9 ± 1.4 |
| **5i** | 87.2 ± 8.0 | 42.0 ± 3.7 | 23.1 ± 4.0 | 12.4 ± 2.7 | 3.3 ± 0.7 |
| **5k** | 83.2 ± 6.7 | 57.0 ± 5.5 | 38.1 ± 5.0 | 22.4 ± 1.7 | 8.3 ± 1.1 |
| **1k + FA** | 83.2 ± 7.0 | 51.4 ± 5.2 | 30.1 ± 2.7 | 14.7 ± 3.0 | 11.0 ± 1.7 |
| **FA** | 79.0 ± 7.6 | 52.2 ± 7.0 | 33.7 ± 1.7 | 15.8 ± 2.0 | 6.6 ± 0.3 |

[a] Data are the mean values ± SEM ($n$ = 3).

## 3. Conclusion

In summary, a series of FA–carbazole hybrid compounds were designed and synthesized with the hope to achieve a synergic action from the antioxidant FA moiety and the ChE inhibitory carbazole moiety. In vitro ChE assay revealed that most of the hybrid compounds showed moderate inhibitory activity against AChE as well as BChE. Particularly, the potency of the inhibition activity of

compound **5k** was even higher than that of the positive control galantamine. The SAR analysis demonstrated that the electron-withdrawing substituent on the carbazole template and the small size of the alkyl substituent on the side chain were beneficial for the ChE inhibition activity. In addition, the target compounds showed pronounced antioxidant ability and neuroprotective property, especially against the $H_2O_2$-induced toxicity. Altogether, the results suggest that the FA–carbazole hybrid compounds, in particular compound **5k**, can be considered as potential therapeutic agents for AD.

## 4. Experimental protocols

### 4.1. Chemistry

#### 4.1.1. Materials and instruments

Melting points were determined using a capillary apparatus (RDCSY-I). All of the compounds synthesized were purified by column chromatography on silica gel 60 (200–300 mesh). IR spectra were measured on KBr pellets with a Nicolet IR200 FTIR spectrometer, and $^1$H NMR spectra were recorded with a Bruker 300/500 MHz spectrometer. Mass spectra were measured on a Bruker Esquire ESIMS instrument. The purity of all tested compounds was characterized by high resolution mass spectrum (Angilent technologies LC/MSD TOF). Individual compounds with the purity of >95% were used for other experiments.

#### 4.1.2. 3-(4-Ethoxycarbonyloxy)-3-methoxyphenyl)acrylic acid (2)

Compound **2** was synthesized using a previous reported method.[1] Generally, to a solution of ferulic acid (5 mmol) in 20 mL 1 M NaOH aqueous solution, ethyl chloridocarbonate (6 mmol) was added dropwise at 5 °C. The mixture was allowed to react for 6 h with stirring at 5 °C. The pH of the mixture was adjusted to 2 with 3 M HCl solution, and white precipitate was formed. Filter, wash with water, and then recrystallize the crude product with acetone to obtain white crystal. Yield 61%, mp 157–158 °C (lit.[1] mp 157–160 °C).

#### 4.1.3. 4-(3-Chloro-3-oxoprop-1-enyl)-2-methoxylphenyl ethyl carbonate (3)

To a solution of compound **2** (1 mmol) in 15 mL anhydrous $CH_2Cl_2$ and 2 drops of DMF, a solution of oxalyl chloride (5 mmol) in 15 mL anhydrous $CH_2Cl_2$ was added dropwise in 0.5 h at 5 °C under $N_2$ atmosphere. Then the mixture was heated to reflux for 3 h to obtain green–yellow solution and concentrated to afford yellow needle solid which was used for the next reaction without purification.

#### 4.1.4. General procedure for the preparation of compounds 5a–k

To a solution of compounds **1a–k** (0.8 mmol) in 30 mL anhydrous $CH_2Cl_2$ and pyridine (1.2 mmol), the solution of flesh compound **3** (1 mmol) in 30 mL anhydrous $CH_2Cl_2$ was added dropwise in 0.5 h at 5 °C. The mixture was stirred for another 3 h at room temperature, concentrated in vacuo and the crude product was purified by column chromatography ($CH_2Cl_2$/EtOAc = 5:1) to give the compounds **4a–k**. Then compounds **4a–k** was dissolved in a mixture of 50 mL of 95% ethanol and 200 μL of aminoethanol and stirred for 12 h at 25 °C. The mixture was concentrated in vacuo, and the residue was diluted with 30 mL water, extracted with $CH_2Cl_2$ (20 mL × 3). The organic layer was dried over anhydrous $Na_2SO_4$, filtered, and concentrated to afford compounds **5a–k**.

**4.1.4.1. *N*-Isopropyl-3-(4-hydroxy-3-methoxyphenyl)-*N*-((7-methoxy-9*H*-carbazol-4-yl)methyl)acrylamide (5a).** Pale yellow solid. mp 98–99 °C. Yield 88%. IR (KBr, cm$^{-1}$): 3207 (OH); 1640 (C=O); 1608, 1579, 1512 (Ar, C=C). $^1$HNMR (500 MHz, $CDCl_3$): $\delta$ 1.26(d, $J$ = 6.9 Hz, 6H), 3.57 (s, 3H), 3.91 (s, 3H), 4.15–4.17 (m, 1H), 5.22 (s, 2H), 6.46 (d, $J$ = 15.2, 1H), 6.60–6.62 (m, 1H), 6.70 (d, $J$ = 7.6 Hz, 1H), 6.78 (d, $J$ = 7.4 Hz, 1H), 6.93 (d, $J$ = 7.4 Hz, 1H), 6.99 (s, 1H), 7.13 (s, 1H), 7.30–7.33 (m, 2H), 7.70 (d, $J$ = 15.2 Hz, 1H), 7.98 (d, $J$ = 7.6 Hz, 1H), 8.37 (s, 1H). HRMS (ESI) $m/z$ Calcd for $C_{27}H_{27}N_2O_4$ $[M-H]^-$ 443.19711 found 443.19786.

**4.1.4.2. *N*-Ethyl-3-(4-hydroxy-3-methoxyphenyl)-*N*-((7-methoxy-9*H*-carbazol-4-yl)methyl)acryl-amide (5b).** White solid. Yield 90%. mp 102–104 °C. IR (KBr, cm$^{-1}$): 3271 (OH); 1642 (C=O); 1609, 1581, 1513 (Ar, C=C). $^1$HNMR (300 MHz, $CDCl_3$): $\delta$ 1.05 (t, $J$ = 6.8 Hz, 3H), 3.59 (s, 3H), 3.93 (s, 3H), 4.30 (q, $J$ = 6.8 Hz, 2H), 5.83 (s, 2H), 6.59 (d, $J$ = 14.1 Hz, 1H), 6.64 (s, 1H), 6.71–6.80 (m, 2H), 6.89–7.02 (m, 3H), 7.33–7.39 (m, 2H), 7.67 (d, $J$ = 14.1 Hz, 1H), 7.99 (d, $J$ = 7.2 Hz, 1H), 8.64 (s, 1H). HRMS (ESI) $m/z$ Calcd for $C_{26}H_{25}N_2O_4$ $[M-H]^-$ 429.18146 found 429.18129.

**4.1.4.3. *N*-Cyclopentyl-3-(4-hydroxy-3-methoxyphenyl)-*N*-((7-methoxy-9*H*-carbazol-4-yl)methyl)acryl-amide (5c).** White solid. Yield 90%. mp 113–115 °C. IR (KBr, cm$^{-1}$): 3239 (OH); 1639 (C=O); 1608, 1579, 1512 (Ar, C=C). $^1$HNMR (300 MHz, $CDCl_3$): $\delta$ 1.56–1.77 (m, 8H), 3.44 (s, 3H), 3.82 (s, 3H), 4.70 (m, 1H), 5.29 (s, 2H), 6.54–6.58 (m, 2H), 6.67 (m, 2H), 6.96–7.10 (m, 5H), 7.77 (d, $J$ = 15.3 Hz, 1H), 8.01 (d, $J$ = 7.5 Hz, 1H), 9.43 (s, 1H). HRMS (ESI) $m/z$ Calcd for $C_{29}H_{29}N_2O_4$ $[M-H]^-$ 469.21256 found 469.21298.

**4.1.4.4. *N*-Cyclohexyl-3-(4-hydroxy-3-methoxyphenyl)-*N*-((7-methoxy-9*H*-carbazol-4-yl)methyl)acryl-amide (5d).** Yellow solid. Yield 86%. mp 96–98 °C. IR (KBr, cm$^{-1}$): 3403 (NH); 3256 (OH); 1639 (C=O); 1609, 1579, 1513 (Ar, C=C). $^1$HNMR (500 MHz, $CDCl_3$): $\delta$ 1.40–1.49 (m, 3H), 1.60–1.63 (m, 2H), 1.74 (m, 3H), 1.91 (m, 2H), 3.59 (s, 3H), 3.91 (s, 3H), 4.77–4.78 (m, 1H), 5.18 (s, 2H), 5.73 (s, 1H), 6.47 (d, $J$ = 15.2 Hz, 1H), 6.61 (s, 1H), 6.70 (d, $J$ = 8.1 Hz, 1H), 6.79 (d, $J$ = 8.0 Hz, 1H), 6.93 (d, $J$ = 8.4 Hz, 1H), 7.00 (s, 1H), 7.14 (d, $J$ = 5.6 Hz, 1H), 7.13 (d, $J$ = 5.6 Hz, 1H), 7.31–7.32 (m, 1H), 7.69 (d, $J$ = 15.2 Hz, 1H), 7.98 (d, $J$ = 8.6 Hz, 1H), 8.36 (s, 1H). HRMS (ESI) $m/z$ Calcd for $C_{30}H_{31}N_2O_4$ $[M-H]^-$ 483.22841 found 483.22846.

**4.1.4.5. *N*-Benzyl-3-(4-hydroxy-3-methoxyphenyl)-*N*-((7-methoxy-9*H*-carbazol-4-yl)methyl)acrylamide (5e).** Yellow solid. Yield 90%. mp 103–106 °C. IR (KBr, cm$^{-1}$): 3398 (NH); 3268 (OH); 1640 (C=O); 1608, 1580, 1512 (Ar, C=C). $^1$HNMR (500 MHz, $CDCl_3$): $\delta$ 3.65 (s, 3H), 3.86 (s, 3H), 4.89 (s, 2H), 5.21 (s, 2H), 5.8 (s, 1H), 6.65 (d, $J$ = 15.1 Hz, 1H), 6.62–7.18 (m, 7H), 7.27–7.33 (m, 6H), 7.72 (d, $J$ = 15.1 Hz, 1H), 7.85 (d, $J$ = 8.6 Hz, 1H), 8.39 (s,1H). HRMS (ESI) $m/z$ Calcd for $C_{31}H_{28}N_2O_4$ $[M-H]^-$ 491.19711 found 491.19730.

**4.1.4.6. *N*-Isopropyl-3-(4-hydroxy-3-methoxyphenyl)-*N*-((9*H*-carbazol-4-yl)methyl)acrylamide (5f).** White solid. Yield 90%. mp 98–100 °C. IR (KBr, cm$^{-1}$): 3268 (OH); 1641 (C=O); 1605, 1580, 1512 (Ar, C=C). $^1$HNMR (500 MHz, $CDCl_3$): $\delta$ 1.25 (d, $J$ = 6.9 Hz, 6H), 3.56 (s, 3H), 5.15 (m, 1H), 5.22 (s, 2H), 5.72 (s, 1H), 6.46 (d, $J$ = 15.1 Hz, 1H), 6.60 (s, 1H), 6.72 (d, $J$ = 7.5 Hz, 1H). 6.78 (d, $J$ = 7.5 Hz, 1H), 6.80 (m, 1H), 7.38 (m, 1H), 7.41 (d, $J$ = 8.0 Hz, 1H), 7.49 (t, $J$ = 7.5 Hz, 8.0 Hz, 2H), 7.54 (d, $J$ = 7.7 Hz, 1H), 7.70 (d, $J$ = 15.1 Hz, 1H), 8.14 (d, $J$ = 7.9 Hz, 1H), 8.44 (s, 1H). HRMS (ESI) $m/z$ Calcd for $C_{26}H_{25}N_2O_3$ $[M-H]^-$ 413.18654 found 413.18676.

**4.1.4.7. *N*-Ethyl-3-(4-hydroxy-3-methoxyphenyl)-*N*-((9*H*-carbazol-4-yl)methyl)acrylamide (5g).** Yellow solid. Yield 82%. mp 110–112 °C. IR (KBr, cm$^{-1}$): 3405 (NH); 3270 (OH); 1642 (C=O); 1606, 1581, 1512 (Ar, C=C). $^1$HNMR (500 MHz, $CDCl_3$): $\delta$ 1.09(t,

$J$ = 6.8 Hz, 3H), 3.58 (s, 3H), 4.39 (q, $J$ = 6.8 Hz, 2H), 5.31 (s, 2H), 6.52 (d, $J$ = 15.2 Hz, 1H), 6.63 (d, $J$ = 1.5 Hz, 1H), 6.72 (d, $J$ = 8.2 Hz, 1H), 6.80 (dd, $J$ = 8.2 Hz, 1.5 Hz, 1H), 7.32 (m, 2H), 7.41 (d, $J$ = 8.0 Hz, 1H), 7.48 (t, $J$ = 7.45 Hz, 8.0 Hz, 2H), 7.53 (d, $J$ = 8.1 Hz, 1H), 7.62 (d, $J$ = 15.2 Hz, 1H), 8.10 (d, $J$ = 8.0 Hz, 1H), 8.33 (s, 1H). HRMS (ESI) $m/z$ Calcd for $C_{25}H_{23}N_2O_3$ $[M-H]^-$ 399.17089 found 399.17066.

**4.1.4.8. *N*-Cyclopentyl-3-(4-hydroxy-3-methoxyphenyl)-*N*-((9*H*-carbazol-4-yl)methyl)acrylamide (5h).** Yellow solid. Yield 91%. mp 115–117 °C. IR (KBr, $cm^{-1}$): 3394 (NH); 3240 (OH); 1640 (C=O); 1605, 1580, 1512 (Ar, C=C). $^1$HNMR (500 MHz, $CDCl_3$): $\delta$ 1.58–1.66 (m, 8H), 3.54 (s, 3H), 4.70 (m, 1H), 5.22 (s, 2H), 5.72 (s, 1H), 6.46 (d, $J$ = 14.9 Hz, 1H), 6.59 (d, $J$ = 1.5 Hz, 1H), 6.70 (d, $J$ = 8.2 Hz, 1H), 6.77 (dd, $J$ = 8.2 Hz, 1.5 Hz, 1H), 7.30 (m, 2H), 7.42 (d, $J$ = 8.0 Hz, 1H), 7.47 (t, $J$ = 7.45 Hz, 8.0 Hz, 2H), 7.51 (d, $J$ = 8.1 Hz, 1H), 7.68 (d, $J$ = 14.9 Hz, 1H), 8.12 (d, $J$ = 8.0 Hz, 1H), 8.45 (s, 1H). HRMS (ESI) $m/z$ Calcd for $C_{28}H_{27}N_2O_3$ $[M-H]^-$ 439.20219 found 439.20253.

**4.1.4.9. *N*-Cyclohexyl-3-(4-hydroxy-3-methoxyphenyl)-*N*-((9*H*-carbazol-4-yl)methyl)acrylamide (5i).** Yellow solid. Yield 92%. mp 112–114 °C. IR (KBr, $cm^{-1}$): 3403 (NH); 3263 (OH); 1641 (C=O); 1606, 1579, 1512 (Ar, C=C). $^1$HNMR (500 MHz, $CDCl_3$): $\delta$ 1.41–1.48 (m, 2H), 1.60–1.63 (m, 3H), 1.74 (m, 3H), 1.91–1.93 (m,2H), 3.57 (s, 3H), 4.78 (m, 1H), 5.25 (s, 2H), 5.68 (s, 1H), 6.47 (d, $J$ = 15.2 Hz, 1H), 6.61 (s, 1H), 6.70 (d, $J$ = 8.2 Hz, 1H), 6.79 (d, $J$ = 7.9 Hz, 1H), 7.18 (s, 1H), 7.33 (t, $J$ = 7.3 Hz, 7.0 Hz, 1H), 7.37 (m, 2H), 7.47 (t, 7.1 Hz, 7.9 Hz, 1H), 7.54 (d, $J$ = 7.9 Hz, 1H), 7.70 (d, $J$ = 15.2 Hz, 1H), 8.13 (d, $J$ = 7.9 Hz, 1H), 8.42 (s, 1H). HRMS (ESI) $m/z$ Calcd for $C_{29}H_{29}N_2O_3$ $[M-H]^-$ 453.21784 found 453.21748.

**4.1.4.10. *N*-Benzyl-3-(4-hydroxy-3-methoxyphenyl)-*N*-((9*H*-carbazol-4-yl)methyl)acrylamide (5j).** Yellow solid. Yield 88%. mp 90–92 °C. IR (KBr, $cm^{-1}$): 3253 (NH, OH); 1641 (C=O); 1582, 1511 (Ar, C=C). $^1$HNMR (300 MHz, $CDCl_3$): $\delta$ 3.58 (s, 3H), 4.99 (s, 2H), 5.34 (s, 2H), 5.48 (s, 1H), 6.68–6.90 (m, 5H), 7.03–7.16 (m, 3H), 7.36–7.51 (m, 6H), 7.85–7.95 (m, 3H), 9.17 (s, 1H). HRMS (ESI) $m/z$ Calcd for $C_{30}H_{25}N_2O_3$ $[M-H]^-$ 461.18654 found 461.18621.

**4.1.4.11. *N*-Ethyl-3-(4-hydroxy-3-methoxyphenyl)-*N*-((7-chloro-9*H*-carbazol-4-yl)methyl)acrylamide (5k).** Yellow solid. Yield 88%. mp 90–92 °C. IR (KBr, $cm^{-1}$): 3255 (OH); 1655 (C=O); 1580, 1515 (Ar, C=C). $^1$HNMR (300 MHz, $CDCl_3$): $\delta$ 1.09 (t, $J$ = 6.9 Hz, 3H), 3.59 (s, 3H), 3.91 (s, 3H), 4.06 (q, $J$ = 6.9 Hz, 2H), 5.22 (s, 2H), 6.49 (d, $J$ = 15.2, 1H), 6.60–6.62 (m, 1H), 6.70 (d, $J$ = 7.6 Hz, 1H), 6.78 (d, $J$ = 7.4 Hz, 1H), 6.93 (d, $J$ = 7.4 Hz, 1H), 6.99 (s, 1H), 7.13 (s, 1H), 7.56–7.59 (m, 2H), 7.78 (d, $J$ = 15.2 Hz, 1H), 7.99 (d, $J$ = 7.6 Hz, 1H), 8.47 (s, 1H). HRMS (ESI) $m/z$ Calcd for $C_{25}H_{22}ClN_2O_3$ $[M-H]^-$ 433.13191 found 433.13166.

### 4.2. Biological studies

#### 4.2.1. Cholinesterase inhibition assay in vitro

The cholinesterase inhibitory activity of the target compounds was measured using Ellman's assay.[2] AChE (E.C.3.1.1.7, Type VI-S, from Electric Eel) and BChE (E.C.3.1.1.8, from equine serum) were purchased from Sigma–Aldrich (Steinheim, Germany). DTNB (Ellman's reagent), ATC and BTC iodides were obtained from Fluka (Buchs, Switzerland). The assay was performed as described in the following procedure: stock solutions of the test compounds were prepared in ethanol, 100 μL of which gave a final concentration of $10^{-3}$ M when diluted to the final volume of 3.32 mL. The highest concentration of the test compounds applied in the assay was $10^{-4}$ M (10% EtOH in the stock solution did not influence enzyme activity). In order to obtain an inhibition curve, at least five different concentrations (normally $10^{-4}$–$10^{-9}$ M) of the test compound were measured at 25 °C at 412 nm, each concentration in triplicate. For buffer preparation, 1.36 g of potassium dihydrogen phosphate (10 mmol) were dissolved in 100 mL of water and adjusted with KOH to pH = 8.0 ± 0.1. Enzyme solutions were prepared to give 2.5 units $mL^{-1}$ in 1.4 mL aliquots. Furthermore, 0.01 M DTNB solution, 0.075 M ATC and BTC solutions, respectively, were used. A cuvette containing 3.0 mL of phosphate buffer, 100 μL of the respective enzyme, and 100 μL of the test compound solution was allowed to stand for 5 min, then 100 μL of DTNB were added, and the reaction was started by addition of 20 μL of the substrate solution (ATC/BTC). The solution was mixed immediately, and exactly 2 min after substrate addition the absorption was measured. For the reference value, 100 μL of water replaced the test compound solution. For determining the blank value, additionally 100 μL of water replaced the enzyme solution. The inhibition curve was obtained by plotting the percentage enzyme activity (100% for the reference) versus logarithm of test compound concentration.

#### 4.2.2. Antioxidant assay in vitro

The experiments of FA and its hybrids to trap galvinoxyl radicals and DPPH radicals were performed following a previous report.[4] DPPH radical (0.1 mM) and galvinoxyl radical (2 μM) were dissolved in ethanol to record the absorbance (Abs0) at 517 and 428 nm, respectively. The concentration ranges of the ethanol solution of the tested compounds are from 1 to 100 μM. The absorbance (Abst) of the mixtures became stable after the tested compounds were added to DPPH radical for 4 h and to galvinoxyl radical for 19 h. The percentages of DPPH radical and galvinoxyl radical scavenged by the tested compounds were calculated by $(1 - \text{Abst}/\text{Abs0}) \times 100$.

#### 4.2.3. Neuroprotective activity in vitro

PC12 cells, obtained from the Cell Bank of the Chinese Academy of Sciences (Shanghai, China), were cultured in a humidified, 5% $CO_2$ atmosphere at 37 °C, and maintained in monolayer culture in F-12 medium supplemented with 10% fetal bovine serum (FBS), 100 mg/mL of streptomycin and 100 mg/mL of penicillin. The cell viability was determined by MTT assay (MTT: 3-(4,5-dimethylthiazol-2-yl)-2,5-diphenyltetrazolium bromide). For the preparation of Aβ42 solution, Aβ42 (Chinapeptides Co., Ltd) was initially dissolved to 1 mM in hexafluoroisopropanol (Sigma) and separated into aliquots in sterile microcentrifuge tubes. Hexafluoroisopropanol was removed under vacuum in a Speed Vac, and the peptide film was stored desiccated at −20 °C. F-12 culture medium was added to bring the peptide to a final concentration of 100 μM and incubated at 4 °C for 24 h. The tested compounds were dissolved in DMSO and diluted to the required concentration with culture medium (DMSO final concentration <0.5%). The suspension of 2000 cells/well was plated in 96-well culture plates with culture medium and was incubated for 24 h at 37 °C, in a 5% $CO_2$ incubator. Then 24 μL of tested compound solution (final concentrations ranging between 0.1 μM and 50 μM), or 24 μL of tested compound solution (final concentrations ranging between 0.1 μM and 50 μM) containing Aβ42 (final concentration 5 μM) or $H_2O_2$ (final concentration 200 μM) was added. Cells were incubated at 37 °C for 24 h. respectively. After that, the cells were treated with 10 mL MTT dye solution (5 mg/mL) for 4 h cultivation. The media with MTT solution were removed with 100 mL of DMSO solution. The absorbance of formazane solution was measured at 540 nm with an automatic microplate ELISA reader. Wells without cells were used as blanks and were subtracted as background from each sample. Results were expressed as a percentage of control. Three independent trials were analyzed and the results were expressed as mean ± SEM.

#### 4.2.4. Molecular modeling and ADME prediction

Homology modeling was carried out using the MOE (Molecular Operating Environment) software (Chemical Computing Group Inc). Initial minimization was performed within the homology modeling function of MOE. The model from MOE was minimized with a few thousand cycles of minimization using the ABNR (adopted-basis Newton–Raphson) method. Ligands were modeled by positioning them in the active site in accordance with the published crystal structures (PDB code: 1P0P and 3I6M). The entire complex was then subjected to alternate cycles of minimization and dynamics. Each dynamics run was short, about 3 ps. The intent was to get a satisfactory structure for the complex that was consistent with the published crystal structure. For the ADME and Toxicity prediction, the compound was firstly sketched using discovery studio 3.0 and then saved as sd format. It was then imported into ADMET predictor 7.0 (Simulation plus, USA) for ADME and toxicity prediction. Calculation was performed under pH = 7.4. Other parameters were set as default. The results were exported into an sd file for further reading.

## Acknowledgments

This work is supported by Natural Science Foundation of Jiangsu Province, China (No. BK20151402) and the Fundamental Research Funds for the Central Universities (No. 3207045413). Dr. Fang is thankful to the support of the Open Project Program of State Key Laboratory of Natural Medicines, China Pharmaceutical University.

## References and notes

1. Cacabelos, R. *Methods Mol. Biol.* **2008**, *448*, 213.
2. Fang, L.; Gou, S.; Fang, X.; Cheng, L.; Fleck, C. *Mini Rev. Med. Chem.* **2013**, *13*, 870.
3. Yang, W.; Wong, Y.; Ng, O. T.; Bai, L. P.; Kwong, D. W.; Ke, Y.; Jiang, Z. H.; Li, H. W.; Yung, K. K.; Wong, M. S. *Angew. Chem., Int. Ed.* **2012**, *51*, 1804.
4. Fang, X.; Fang, L.; Gou, S.; Lupp, A.; Lenhardt, I.; Sun, Y.; Huang, Z.; Chen, Y.; Zhang, Y.; Fleck, C. *Eur. J. Med. Chem.* **2014**, *76*, 376.
5. Markesbery, W. R.; Carney, J. M. *Brain Pathol.* **1999**, *9*, 133.
6. Picone, P.; Bondi, M. L.; Montana, G.; Bruno, A.; Pitarresi, G.; Giammona, G.; Di Carlo, M. *Free Radical Res.* **2009**, *43*, 1133.
7. Saxena, A.; Redman, A. M. G.; Jiang, X.; Lockridge, O.; Doctor, B. P. *Biochemistry* **1997**, *36*, 14642.
8. Greenblatta, H. M.; Krygera, G.; Lewis, T.; Silman, I.; Sussman, J. L. *FEBS Lett.* **1999**, *463*, 321.
9. Feng, J. Y.; Liu, Z. Q. *J. Agric. Food Chem.* **2009**, *57*, 11041.
10. Shi, Y. F.; Zhang, H. Y.; Wang, W.; Fu, Y.; Xia, Y.; Tang, X. C.; Bai, D. L.; He, X. C. *Acta Pharmacol. Sin.* **2009**, *30*, 1195.
11. Jakob-Roetne, R.; Jacobsen, H. *Angew. Chem., Int. Ed.* **2009**, *48*, 3030.